Coexistence in the even zinc isotopes

M. Carchidi* and H. T. Fortune
Department of Physics, University of Pennsylvania, Philadelphia, Pennsylvania 19104
(Received 1 May 1987)

A generalized two-state coexistence model developed to describe the $0^{+'}$ to ground state cross-section ratios in the (p,t) and (t,p) reactions on even-even nuclei is applied to the zinc isotopes. We demonstrate that two-state mixing wave functions for the ground state and excited $0^{+'}$ state in ^{A}Zn can quantitatively account for all $\sigma(0^{+'})/\sigma$ (g.s.) ratios in Zn(p,t) and Zn(t,p). Finally, we couple these 0^{+} wave functions with a set of two-state mixing 2^{+} wave functions to describe the $E2$ transition-rate data in ^{68}Zn.

I. INTRODUCTION

It is well known that the direct-reaction process is not restricted to single-particle transfer. Specifically, the shapes of angular distributions resulting from the transfer of two neutrons [i.e., (p,t) and (t,p)] are, in most cases, accounted for by distorted-wave Born-approximation (DWBA) calculations. If spin-orbit forces are neglected, the cross section for two-nucleon transfer can be written as[1]

$$\sigma(\theta)=\sum_{SJTLL_z} f(S,T)\left|\sum_{\rho\lambda} S^{1/2}(\rho\lambda;JT)B(LL_z\theta EQ)\right|^2, \tag{1}$$

where the kind of reaction [i.e., (p,t) or (t,p)] enters into the function $f(S,T)$. The kinematics of the reaction (i.e., the scattering angle θ, the beam energy E, and the Q value Q) enters through the transfer-amplitude function $B(LL_z\theta EQ)$. All nuclear structure information is contained in the spectroscopic amplitudes $S^{1/2}(\rho\lambda;JT)$. Unlike the simplicity in single-particle transfer, the summation in Eq. (1) over the shell-model orbits ρ and λ of the transferred pair makes it not possible to factor the cross section into the nuclear structure part $S^{1/2}(\rho\lambda;JT)$ and the nuclear reaction part $B(LL_z\theta EQ)$. For this reason, any comparison between experiment and theory requires the existence of some nuclear model space and interaction (i.e., a shell-model Hamiltonian and initial- and final-state wave functions) to calculate the spectroscopic amplitudes *and* a set of optical-model parameters and potentials to calculate the transfer amplitudes. Moreover, the final calculated cross sections are very sensitive to the details of the shell-model Hamiltonian and thus very model dependent.

For nuclei beyond the *sd* shell, there exist very few systematic shell-model calculations which fit the experimental energy levels over an extensive range of nuclei. Moreover, many of the existing calculations cannot account for the energy levels of the so-called "intruder" states. These intruder states are not present in a typical "reasonably sized" shell-model space. Of course, one can always enlarge the model space to include these intruders, but then the calculation would become impractical. In this paper, we are concerned with the two-neutron pickup and stripping reactions to the ground state and low lying excited $0^{+'}$ intruder state in the residual nucleus. Cross sections as described in Eq. (1) cannot be calculated for these states since they are not present in the shell-model space. In an attempt to study these intruder states, we investigate the possibility of quantitatively describing the $0^{+'}$/g.s. (p,t) and (t,p) cross-section ratios using a two-state coexistence model and assuming as little as possible about the initial- and final-state model wave functions.

II. THE MODEL

We report herein on a two-state coexistence model analysis of (p,t) and (t,p) data on even zinc isotopes. The model, hereinafter referred to as Rerg1, has been developed in detail[2] and applied successfully[2,3] to even germanium isotopes. Briefly, the physical ground state and excited $0^{+'}$ states are given in terms of basis states ϕ_g^A and ϕ_e^A by the general relations

$$\Psi^A(\text{g.s.})=\alpha_A\phi_g^A+\beta_A\phi_e^A$$

and (2)

$$\Psi^A(0^{+'})=\beta_A\phi_g^A-\alpha_A\phi_e^A$$

with α_A and β_A assumed real and $\alpha_A^2+\beta_A^2=1$. Two-neutron transfer amplitudes connecting the basis states are as depicted in Fig. 1. The two-neutron transfer amplitude ratios r_A, s_A, and R_A are assumed real, independent of A and equal in pickup and stripping (i.e., $r_A=r=s_A=s$ and $R_A=R$). The basis states are not otherwise specified. The calculated $0^{+'}$/g.s. cross-section amplitude ratios, denoted by $|T_A|$ for stripping and $|P_A|$ for pickup (where A is the lighter of target and residual nuclei) are then given by

$$|T_A|=\left|\frac{x_A+r(1-x_Ax_{A+2})-x_{A+2}R}{x_Ax_{A+2}+r(x_A+x_{A+2})+R}\right| \tag{3a}$$

and

$$|P_A|=\left|\frac{x_{A+2}+r(1-x_Ax_{A+2})-x_AR}{x_Ax_{A+2}+r(x_A+x_{A+2})+R}\right|, \tag{3b}$$

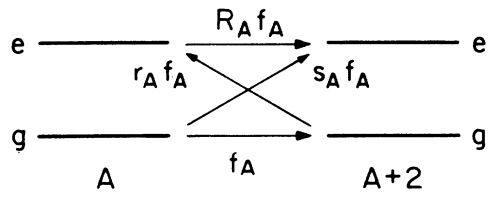

FIG. 1. Basis state definitions of r_A, s_A, and R_A.

where $x_A = \alpha_A/\beta_A$.

It is seen through DWBA calculations for two-neutron transfer (assuming the same two-neutron bound-state wave function for the ground state and $0^{+'}$ state), that there is very little difference in phase between $[\sigma_{\mathrm{DWBA}}(\mathrm{g.s.}\rightarrow\mathrm{g.s.})]^{1/2}$ and $[\sigma_{\mathrm{DWBA}}(\mathrm{g.s.}\rightarrow 0^{+'})]^{1/2}$. This result is consistent with the assumption that α_A, β_A, r, and R are real and it allows one to require also that P_A and T_A are real.

For this model to be consistent with the $\sigma(0^{+'})/\sigma(\mathrm{g.s.})$ data, it is both *necessary* and *sufficient* that the data satisfy the conditions[2]

$$L_A \equiv \frac{(T_{A+2}-P_A)(T_{A-2}-P_A)(1+T_A^2)}{(P_{A+2}-T_A)(P_{A-2}-T_A)(1+P_A^2)} = 1 \quad (\text{for all } A) , \tag{4}$$

which leads to the constant equation

$$r^2 = R + K_A(R+1)^2 . \tag{5}$$

Here K_A is determined completely by the data, is independent of A, is negative, and has the form

$$K_A = \frac{(P_{A-2}-T_A)(T_{A-2}-P_A)}{(P_A P_{A-2}-T_A T_{A-2})^2+(P_A+P_{A-2}-T_A-T_{A-2})^2} . \tag{6}$$

The mixing amplitudes α_A and β_A can then be determined in terms of the single parameter R, which is mathematically restricted only by the bounds of the ellipse (since $K_A<0$) of Eq. (5) when viewed on an R-r plane. One notes from Eq. (6) that $1+4K_A \geq 0$ and so R can always be chosen to lie near unity and solutions for both r positive and r negative are allowed. We choose a phase convention in which all the x_A's are non-negative. Thus, for complete constructive interference in the $\Psi^A(\mathrm{g.s.})\leftrightarrow\Psi^{A+2}(\mathrm{g.s.})$ two-neutron transfer overlaps, one would expect r to be non-negative. Of course, by assuming that $r=s$, one can always transform, by a change of basis to the basis set that has $r\equiv 0$. However, this choice of basis may not always be consistent with the above phase requirement. This phase convention can further restrict the values of the parameter R beyond those already required by the elliptic nature of Eq. (5). We also define the mixing potential $U_A = -E_A\alpha_A\beta_A$ (E_A in nucleus A being the excitation energy of the physical $0^{+'}$ state relative to the physical ground state and always positive). In terms of x_A, $U_A = -E_A x_A/(1+x_A^2)$ and is well defined everywhere and (under our phase convention) is aways non-positive.

The method for constructing the mixing probabilities for the wave functions in Eq. (2) is then to start with the data points and their uncertainties (denoted by $T_{A_0}\pm\Delta T_{A_0}$ and $P_{A_0}\pm\Delta P_{A_0}$), and deduce the "best-fit" cross-section ratios (denoted by T_A and P_A) by minimizing the least squared function

$$\chi^2 = \left[\frac{A''-A'+2}{2}\right]^{-1} \sum_{A=A'}^{A''} \{[(P_A-P_{A_0})/\Delta P_{A_0}]^2 + [(T_A-T_{A_0})/\Delta T_{A_0}]^2\} , \tag{7}$$

subject to the $(A''-A'+2)/2$ conditions that $L_A=1$ for $A=A'+2, A'+4, \ldots, A''-2$. A "good" fit occurs when χ^2 is small and the smallest χ^2 will determine the best-fit values of T_A and P_A and their signs. The values of x_A and, hence, α_A^2 (or $\beta_A^2 = 1-\alpha_A^2$) are obtained in terms of R by the equations provided in Ref. 2. In addition, it was shown in detail[2] that not all solutions obtained this way are independent. They are related through reflections of the form $r\leftrightarrow -r$, $R\leftrightarrow 1/R$, and $(P_A, T_A)\leftrightarrow(-P_A, -T_A)$. Through these symmetries, the number of *independent* solutions is reduced by at least a factor of 4.

The simple-model limit (SML), for which $R\equiv 1$ and $r\equiv 0$, was explored by Vergnes[4] and others.[5] This limit can be physically realized, for example, when ϕ_e^A represents a two-phonon excited state in the vibrational limit and ϕ_g^A represents a zero-phonon ground state, or, for example, when ϕ_e^A contains no two-neutron excitations from ϕ_g^A. In the former case, ϕ_e^A and ϕ_g^A are contained in the same model space and so ϕ_e^A is not an intruder state, while in the latter case, ϕ_e^A is an intruder state since it is not contained in the same model space as ϕ_g^A. The SML was shown[4] to approximate the ^{72}Ge data, but (as we shall see later) is not at all appropriate for any of the zinc isotopes. The Rerg1 model allows one to fit the $\sigma(0^{+'})/\sigma(\mathrm{g.s.})$ data for an entire string of isotopes in even-even nuclei. In practice, the value of $1+4K_A$ in the Rerg1 model is very nearly zero leading to $R\approx 1$ and $r\approx 0$. We define as the approximate simple-model limit (ASML), that set of signs for which r is small and R is near unity, in which case (since $1+4K_A\approx 0$) we must have $T_A+P_A\approx 0$, or $T_A P_A<0$ for all A. That is, the signs taken from Eqs. (3a) and (3b) should be opposite for pickup and stripping. This limit can also be physically realized, for example, when ϕ_e^A and ϕ_g^A represent small deviations from a two-phonon

and zero-phonon vibrational state, respectively, or for example, when ϕ_e^A contains small two-neutron excitation configurations from ϕ_g^A.

III. SELECTION OF THE ZINC DATA

In the above Rerg1 model, the physical ground state and physical excited $0^{+'}$ state result from mixing between the basis ground and excited states. It is not always transparent which excited $0^{+'}$ state is mixed with the ground state. Some guidance in choosing the mixed excited $0^{+'}$ state[6] can be found in the A dependence of the energy for the excited $0^{+'}$ state. Specifically, the excitation energy of the mixed excited $0^{+'}$ state should, as a function of mass number A, be high for the lighter isotopes, reach a minimum around midshell, and then increase again for the heavier isotopes.[6] As mentioned earlier, since the mixed excited $0^{+'}$ state is an intruder state, it should not be reproduced in a simple shell-model calculation. For the zinc isotopes, shell-model calculations have been performed[7] using the unrestricted $1p_{3/2}$-$0f_{5/2}$-$1p_{1/2}$ model space (i.e., closed ^{56}Ni core) and an effective Hamiltonian obtained[8] by Koops and Glaudemans from a fit to low-lying nickel and copper level energies. Their results show that the first excited 0^+ states are correctly predicted in ^{62}Zn and ^{64}Zn, but are calculated too high for the heavier-mass zinc isotopes. Therefore in ^{62}Zn and ^{64}Zn, there may exist an ambiguity as to the correct excited 0^+ state to be used in the present Rerg1 model. Usually one chooses the first excited 0_2^+ state as the mixed state since it is the closest in energy to the ground state and thus would require a smaller potential for the mixing. However, in some cases, the next excited 0^+ state, 0_3^+, is a better choice. This ambiguity exists, for example, in the ^{76}Ge nucleus,[3] where 0_3^+ appears appropriate. Figure 2 gives a plot of the low-lying positive parity states[9] in the even zinc isotopes. Therefore, using the guidelines from Refs. 6 and 7, the choice of the 0_2^+ state as the mixed state in $^{66-72}$Zn is reasonable. However, in ^{64}Zn it is not clear which excited $0^{+'}$ state to use (either the 0_2^+ level at 1.910 MeV, the 0_3^+ state at 2.609 MeV, or even the 0_4^+ state at 3.240 MeV). Of course, the "V-shaped" excitation energy dependence in the intruder 0^+ level would

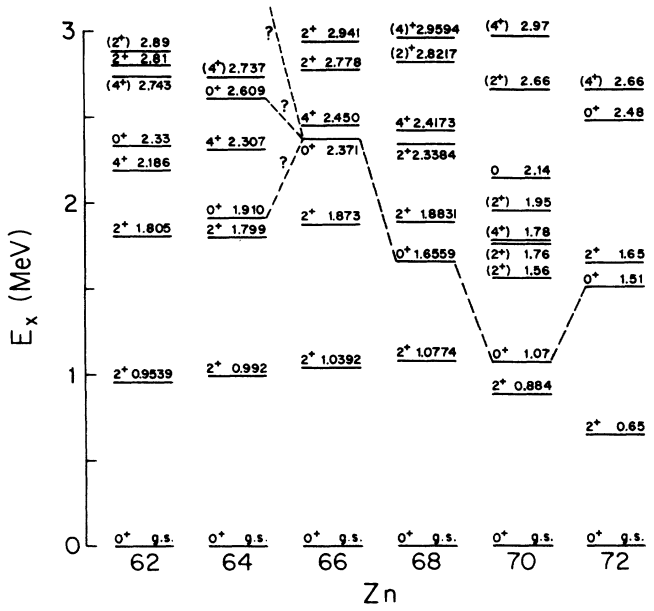

FIG. 2. Low-lying positive-parity states of even-even zinc isotopes.

favor using the 0_4^+ as the excited $0^{+'}$ state to be mixed with the ground state in a two-state mixing model. However, for completeness, we shall consider calculations using all three of these excited 0^+ states in ^{64}Zn.

As can be seen in Eq. (4), a complete description of (t,p) and (t,p) data using the Rerg1 model requires the knowledge (for a given A_0) of at least six data points of the form $P^2_{(A-2)_0}$, $P^2_{A_0}$, $P^2_{(A+2)_0}$, $T^2_{(A-2)_0}$, $T^2_{A_0}$, and $T^2_{(A+2)_0}$. If we assume that the mixed excited $0^{+'}$ state is the *first* excited 0^+ state, then for the zinc isotopes there exists in the literature[10–13] the measured values of P^2_{64}, P^2_{66}, T^2_{64}, T^2_{66}, and T^2_{68}. The ^{70}Zn(p,t)^{68}Zn reaction has been measured[14] at 17.5-MeV proton energy, but the poor resolution of the data and the presence of ^{68}Zn in the ^{70}Zn target did not allow a complete separation of the 0_2^+ level (at 1.656 MeV) in ^{68}Zn from the ground state of ^{66}Zn and, therefore, the $\sigma(0_2^+)/\sigma$(g.s.) ratio was not determined. We have measured the ^{70}Zn(p,t)^{68}Zn re-

TABLE I. Experimental cross-section ratios for $2n$ pickup and stripping on even zinc isotopes.

	$\sigma_{exp}(0_2^+)/\sigma_{exp}$(g.s.)		
	(p,t)		(t,p)
A[a]	$E_p=35$ MeV[b]	$E_p=51.9$ MeV[c]	$E_t=12$ MeV[d]
62	0.0016±0.0002	0.0025±0.0006	
64	0.006 ±0.0012	0.0077±0.0019[e]	0.0114±0.0023
66		0.0490±0.0147[e]	0.0123±0.0018
68	0.1812±0.0091[f]		0.0374±0.0056
70			0.1145±0.0172

[a] A is the target nucleus for (t,p) and the residual nucleus for (p,t).
[b] Reference 11 ($\theta_{c.m.}=20°$).
[c] Reference 10.
[d] Reference 12.
[e] Angle integrated cross sections taken from Ref. 10.
[f] Reference 15.

TABLE II. Optical-model parameters used in the DWBA analysis.[a]

	V (MeV)	r_0 (fm)	a (fm)	W (MeV)	$W'=4W_D$ (MeV)	r_0' (fm)	a' (fm)	r_0 (fm)
p	50.5	1.15	0.65		60.0	1.25	0.47	1.30
t	168.0	1.20	0.65	13.5		1.60	0.87	1.30

[a]From J. F. Mateja *et al.*, Phys. Rev. C **17**, 2047 (1978), except for the change $r_0=1.15$ for protons.

action[15] using a 35-MeV proton beam generated from the Princeton Cyclotron and have determined a precise value for P^2_{68}, thus completing the six data points necessary to do a Rergl analysis of zinc.

The resulting measured cross-section ratios, $P^2_{A_0}$ and $T^2_{A_0}$, to be considered in our analysis are summarized in Table I. In that table the $T^2_{A_0}$ data were all measured at a forward angle ($\theta_{\text{c.m.}}\approx 5.1°$). The $P^2_{A_0}$ results are from data at 20° because data for all nuclei do not exist at forward angles, and in most cases the cross section at 20° is larger than that at forward angles which means that the ratio $P^2_{A_0}$ is better determined. In addition we found Zn(p,t) data measured at $E_p=35$, 51.9, and 55.12 MeV. For the case of the ^{66,68}Zn(p,t)^{64,66}Zn reactions at 51.9 MeV, the $\sigma(0_2^+)/\sigma$(g.s.) ratios are from angle-integrated yields. The kinematic differences between the measurements at $E_p=35$ MeV and $E_p=51.9$ MeV show why it is important to remove kinematic A dependent in these cross-section ratios before we can proceed with the Rergl analysis. To correct the data for these "Q-value" effects, DWBA calculations were performed with the code DWUCK (Ref. 16) using the optical-model parameters in Table II and a mixed configuration form factor[17] containing the $2p_{1/2}$, $1f_{5/2}$, and $1g_{9/2}$ orbitals. The optical-model parameters in Table II were chosen because they fit[15] the angular distributions in the ^{70}Zn(p,t)^{68}Zn reaction. Calculations were performed for all beam energies (in accordance with the kinematic-correction procedure described in Refs. 2 and 3) at which the experimental numbers were measured. Ratios of DWBA cross sections are summarized in Table III.

TABLE III. DWBA calculated cross-section ratios for $2n$ pickup and stripping on even zinc isotopes using the same mixed configuration $2n$ bound-state wave function for the ground state and $0^{+'}$ state.

	$\sigma_{\text{DWBA}}(0_2^+)/\sigma_{\text{DWBA}}$(g.s.) (p,t)[a]		(t,p)[b]
A	$E_p=35$ MeV	$E_p=51.9$ MeV	$E_t=12$ MeV
62	0.844	1.135	
64	0.957	1.117	1.099
66		1.156	1.021
68	1.034		0.991
70			0.942

[a]Ratio of the 20° points.
[b]Ratio of the 0° points.

We note that these ratios are very nearly unity in all cases. This results from the fact that the same mixed configuration form factor is used in both the g.s.→g.s. transfer and the g.s.→0^+ transfer. In this way, we can remove from the experimental cross-section ratios those effects due only to Q-value differences. To investigate configuration dependences in the DWBA calculations, we also ran the code DWUCK for bound states of pure $(1g_{9/2})^2_0$ and of pure $(2p_{1/2})^2_0$, and we used these results to estimate the uncertainties in the DWBA ratios. The final Q-corrected ratios, along with their uncertainties to be used in the Rergl analysis, are summarized in Table IV and are plotted versus neutron number N in Fig. 3. Also in this figure are the Q-corrected $0^{+'}$/g.s. cross-section ratios from the germanium data used in Ref. 3. The similarity of the two sets of ratios may imply that the "neutron" part of the wave functions for the ground states and $0^{+'}$ states in germanium and zinc are similar.

IV. THE Rergl ANALYSIS ON THE ZINC ISOTOPES USING THE 0_2^+ STATES AS THE MIXED-EXCITED $0^{+'}$ STATES

When a least-squared minimization of Eq. (7) is performed on the zinc data, many possible signs in P_A and T_A yield a small value for χ^2. Of these, only two *independent* solutions satisfy the ASML. These correspond to the following. (a) all P_A negative and all T_A positive (denoted by calculation No. 1), yielding $\chi^2\approx 0.1$ and 2) that where P_{64}, T_{66}, and T_{68} are negative with

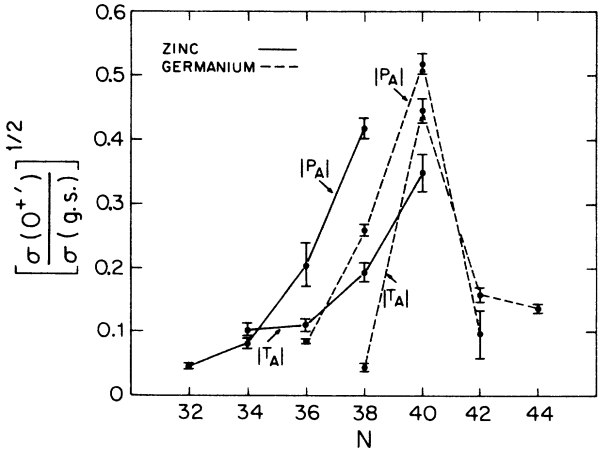

FIG. 3. Experimental $|P_{A_0}|$ and $|T_{A_0}|$ ratios vs neutron number N, in zinc and germanium.

TABLE IV. Cross-section ratios corrected for Q value (Expt./DWBA).

	$P^2_{A_0}$ [a]		$T^2_{A_0}$
A	$E_p=35$ MeV	$E_p=51.9$ MeV	$E_t=12$ MeV
62	0.0019±0.0003	0.0022±0.0006	
64	0.0063±0.0013	0.0069±0.0019	0.0104±0.0021
66		0.0424±0.0140	0.0121±0.0021
68	0.175 ±0.0123		0.0377±0.0057
70			0.122 ±0.020

[a]The $P^2_{A_0}$ numbers to be used in the analysis are the averages of the 35-MeV and 51.9-MeV points, whenever both exist.

the rest all positive (denoted by calculation No. 2) giving $\chi^2\approx 0.4$. In both cases, in order to fulfill the phase requirement $x_A \geq 0$ (or $-U_A \geq 0$) for all A from 64 to 70, it was necessary to require r negative. The plots of α^2_A and $-U_A$ versus R for the various calculations are given in Figs. 4–7. As mentioned earlier, a negative r value indicates destructive interference in the physical g.s. to g.s. $2n$-transfer overlaps in the sense that the expression for $\sigma[{}^AX(\mathrm{t,p}){}^{A+2}X(\mathrm{g.s.})]$ does not contain all positive terms. The germanium analysis of Ref. 3 had r positive indicating constructive interference in the physical g.s. to g.s. $2n$-transfer overlaps. A look at Figs. 5 and 7 shows that for both calculations, the physical region for R (that region where all x_A's are non-negative or, equivalently, all $-U_A$'s are non-negative) is almost the entire mathematical region determined by the elliptic nature of r and R [Eq. (5) with K_A negative]. The plots of α^2_A (Figs. 4 and 6) for each calculation show that the mixture of the basis states for ^{70}Zn (i.e., α^2_{70}) is different from that of the lighter isotopes (i.e., α^2_{64-68}). This result is consistent with the suggestion[4] that there exists a transition with A in the zinc isotopes with the "point of transition" occurring at $N=40$ and with an earlier analysis[18] of the $^{A-4}$Zn(^{6}Li,d)^{A}Ge reactions. A similar transition exists in the Rergl study of the germanium isotopes[3] also at $N=40$.

The two-state Rergl analysis produces a continuous family of solutions all expressible in terms of the single parameter R. No one particular R value is preferred unless we rely on other information. A look at Fig. 7 shows that for calculation No. 2, we could "almost" require the mixing potentials for each isotope to be equal (at about -0.49 MeV). With this requirement, calculation No. 2 would "prefer" an R value of 0.688. Calculation No. 1 (Fig. 5), on the other hand, would give three mixing potentials almost equal to -0.485 MeV at around $R=1.416$. The values of K_A in both calculations are very nearly equal to the simple limit of $-\frac{1}{4}$, but their uncertainties do not overlap this simple-model limit. Therefore a SML-type analysis here will not fit the data. This fact is also especially evident from the observation that none of the zinc data satisfies $P^2_A=T^2_A$, a necessary requirement for the SML to work.

In the ASML discussed above, we required P_A and T_A to have different signs in order for P_A+T_A to be "small." If, however $|P_A|$ and $|T_A|$ are both small, their sum is small for any choice of sign. In the case of zinc, both $|P_{64}|$ and $|T_{64}|$ are small and if we drop the restriction of $P_{64}T_{64}$ negative, then there exists another acceptable Rergl solution ($\chi^2\approx 1.5$) to the $2n$-transfer data (denoted by calculation No. 3). This corresponds to having T_{66} and T_{68} positive, and all the rest

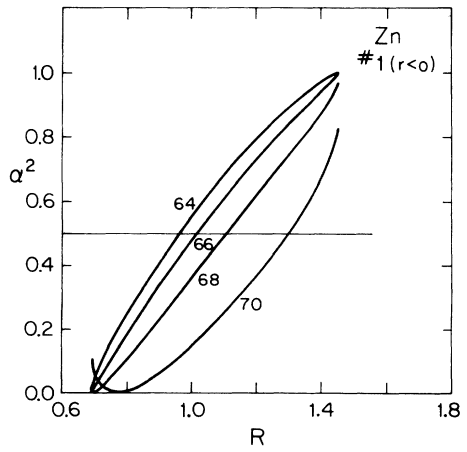

FIG. 4. Plot of α^2_A vs R for calculation No. 1 and r negative.

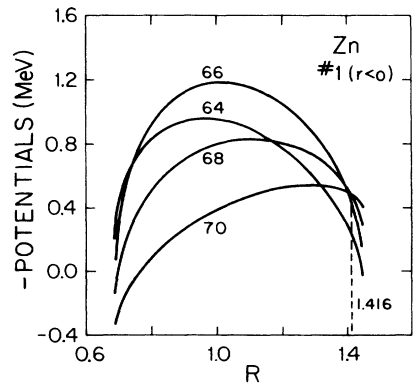

FIG. 5. Plot of $-U_A$ (in MeV) vs R for calculation No. 1 and r negative.

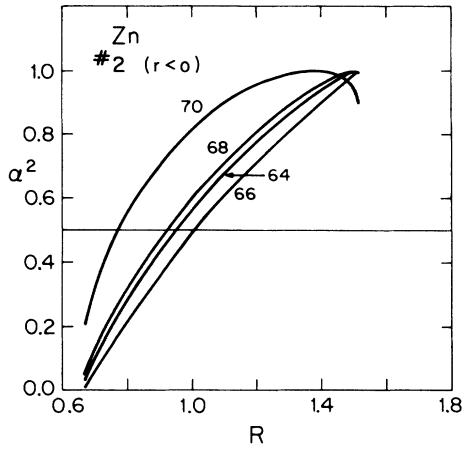

FIG. 6. Plot of α_A^2 vs R for calculation No. 2 and r negative.

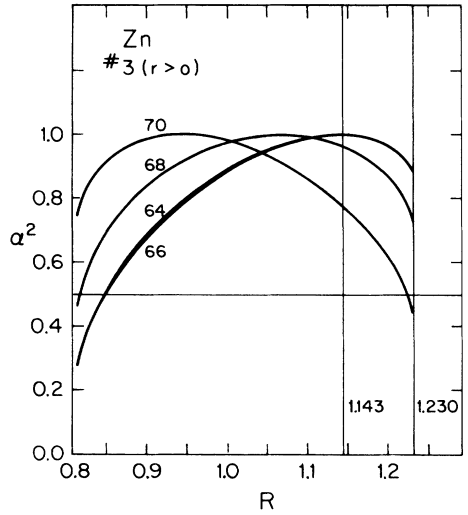

FIG. 8. Plot of α_A^2 vs R for calculation No. 3 and r positive showing the physical region between the broad vertical lines.

negative. The plots of α_A^2 and $-U_A$ for this case are given in Figs. 8 and 9. Here, it is possible to allow all x_A's (or $-U_A$'s) to be non-negative and leave r positive. The results, however, lead to a narrow physical range of $1.14 \leq R \leq 1.23$, as shown in Fig. 9 by the vertical bars. The α_A^2's for this solution (Fig. 8) show $\alpha_{64}^2 \approx \alpha_{66}^2$ for all R and α_{70}^2 again different from the other three. In addition, even here we could almost make all potentials agree at around $R=1.21$.

The results of all three calculations in this section are summarized in Tables V and VI. The K_A values for all three calculations are very near their minimum value of $-\frac{1}{4}$, especially the K_A value in calculation No. 3 which is given by -0.2473 ± 0.0026. In this sense, calculation No. 3 just misses the SML. One must be reminded (as discussed in Ref. 2) that K_A is a very sensitive measure of the SML of $R \equiv 1$ and $r \equiv 0$ (i.e., $P_A = -T_A$). More precisely, if the value of K_4 *does not* overlap $-\frac{1}{4}$, then the SML of Vergnes *will not* fit all the (p,t) and (t,p) data for the entire isotopic string. However, if the value of K_A *does* overlap the simple limit of $-\frac{1}{4}$, we are *still not* guaranteed that the SML will work. In this case, one must instead check to see if $P_A + T_A = 0$ for all A. In other words, the SML will fit the data *if and only if* $P_A + T_A = 0$ within the experimental uncertainties for all A.

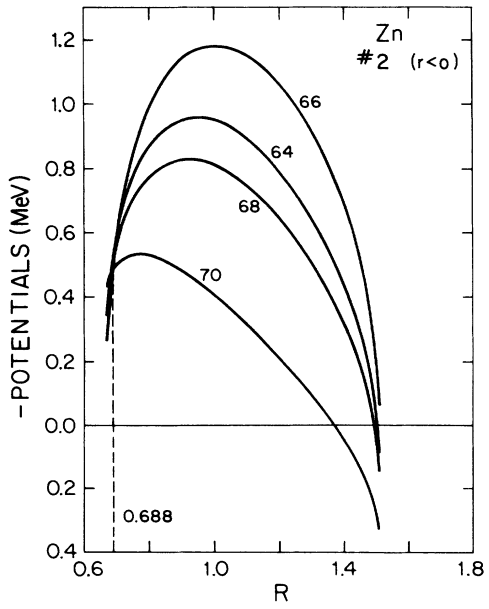

FIG. 7. Plot of $-U_A$ (in MeV) vs R for calculation No. 2 and r negative.

A. Wave functions for ^{62}Zn and ^{72}Zn

The least-squares minimization procedure of Eq. (7) allows one to determine sign choices of P_{64}, P_{66}, P_{68},

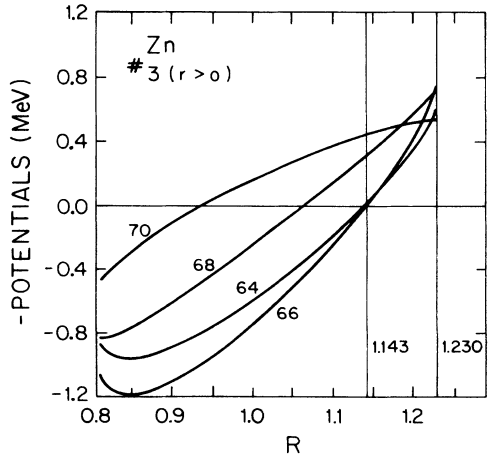

FIG. 9. Plot of $-U_A$ (in MeV) vs R for calculation No. 3 and r positive showing the physical region between the broad vertical lines.

TABLE V. Experimental and calculated cross-section ratios along with the K_A values[a,b] for calculations 1 and 2.

	Experimental values		Calculated values Calc. No. 1		Calc. No. 2	
A	$\lvert P_{A_0}\rvert \pm\Delta P_{A_0}$	$\lvert T_{A_0}\rvert \pm\Delta T_{A_0}$	P_A	T_A	P_A	T_A
62	0.045±0.006		±0.045		±0.045	
64	0.081±0.013	0.102±0.010	−0.083	0.101	−0.076	0.105
66	0.206±0.034	0.110±0.010	−0.182	0.112	0.168	−0.118
68	0.419±0.015	0.194±0.015	−0.420	0.192	0.420	−0.193
70		0.349±0.029		±0.349		±0.349

[a] $K_A = -0.2415\pm0.0037$ for calculation No. 1.
[b] $K_A = -0.2397\pm0.0022$ for calculation No. 2.

T_{64}, T_{66}, and T_{68}. Knowledge of P_{62_0} (Refs. 10 and 11) and T_{70_0} (Ref. 12) permits one to calculate wave functions for ^{62}Zn and ^{72}Zn via Eqs. (36) and (37) of Ref. 2. There is, however, an ambiguity in the signs of P_{62} and T_{70} which is not determined by any of the Rerg1 analysis. We shall therefore consider only calculation No. 1 and make the natural assumption that P_{62} is negative and T_{70} is positive thus allowing for all P_A negative and all T_A positive. Also for this reason we calculate only the α_A^2's and not the mixing potentials. The results are shown in Fig. 10 and if one overlaps this figure with Fig. 4, it becomes clear from the difference in shapes between $\alpha^2_{64,66,68}$ and $\alpha^2_{70,72}$ that a transition in the mixing probabilities is occurring at $N=40$. This result is in further agreement with the belief that the light isotopes of zinc behave one way and the heavier ones another, with a transition occurring between ^{68}Zn and ^{70}Zn (i.e., $N=40$).

B. The excited 0^+ states in ^{64}Zn

The germanium isotopes reveal a roughly V-shaped trend in the excitation energy E_A of the excited 0^+ state which is mixed with the ground state as seen in Fig. 3 of Ref. 2. The minimum of E_A occurs at ^{72}Ge or $N=40$, about where the transition between the lighter and heavier isotopes occurs. With zinc, a similar feature emerges as seen in Fig. 2. Around $N=40$, the place where the shape of the α_A^2's changes, there is a minimum in E_A, although not as dramatic here as in germanium—i.e., the 0_2^+ state in ^{70}Zn is not its first excited state. As mentioned earlier, a reliable signature[6] for choosing the mixed excited $0^{+'}$ state can be found in the energy level spectrum in that the plot of E_A versus A should be high for the lighter isotopes, reach a minimum, and then increase for higher A. The 1.910-MeV state in ^{64}Zn violates this A-dependent trend in that it is too low in excitation. This is one reason why the plot of $-U_{64}$ in Fig. 5 falls below the other three curves at $R=1.416$. These results lead one to investigate what changes, if any, would result if the 2.609-MeV or the 3.240-MeV state in ^{64}Zn were to be chosen as the excited $0^{+'}$ mixed state. Both states are seen[11] in ^{68}Zn(p,t)^{64}Zn. The Q-corrected values for $P^2_{64_0}$ are 0.0206±0.0018 for the 2.609-MeV state and 0.0149±0.0015 for the 3.240-MeV state. In both of these cases, we shall require the ASML condition that $P_{64}T_{64}$ is negative because $\lvert P_{64}\rvert$ can no longer be considered small.

A Rerg1 calculation was performed for both cases of $E_{64}=2.609$ and 3.240 MeV. In both calculations, only that sign combination where $T_A>0$ and $P_A<0$ gives acceptable fits ($\chi^2=0.06$ for the 2.609-MeV calculation and $\chi^2=0.003$ for the 3.240-MeV calculation). Table VII summarizes the results of each calculation and Figs. 11–14 give the plots of α_A^2 and $-U_A$ versus R. In both cases, we must still require r to be negative and the general shapes of α_A^2 are not changed and are similar to the results in Figs. 4 and 10. The plots of $-U_A$ versus R in Figs. 12 and 14 show congestion around $R=1.298$ for

TABLE VI. Experimental and calculated cross-section ratios along with the K_A value[a] for calculation No. 3.

	Experimental values		Calculated values Calc. No. 3	
A	$\lvert P_{A_0}\rvert \pm\Delta P_{A_0}$	$\lvert T_{A_0}\rvert \pm\Delta T_{A_0}$	P_A	T_A
62	0.045±0.006		±0.045	
64	0.081±0.013	0.102±0.010	−0.079	−0.095
66	0.206±0.034	0.110±0.010	−0.304	0.106
68	0.419±0.015	0.194±0.015	−0.416	0.198
70		0.349±0.029		±0.349

[a] $K_A = -0.2473\pm0.0026$ for calculation No. 3.

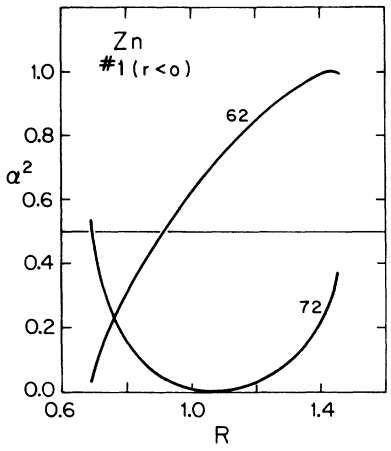

FIG. 10. Plot of α_{62}^2 and α_{72}^2 vs R, assuming all P_A negative and all T_A positive and r negative.

TABLE VII. Summary of calculated cross-section ratios using E_{64} equal to 2.609 and 3.240 MeV.

	$E_{64}=2.609$ MeV[a]		$E_{64}=3.240$ MeV[b]	
A	P_A^2	T_A^2	P_A^2	T_A^2
62	0.0021		0.0021	
64	0.0206	0.0106	0.0149	0.0104
66	0.0506	0.0118	0.0441	0.0120
68	0.1745	0.0383	0.1753	0.0370
70		0.1216		0.1216

[a] $K_A = -0.2454 \pm 0.0040$.
[b] $K_A = -0.2443 \pm 0.0040$.

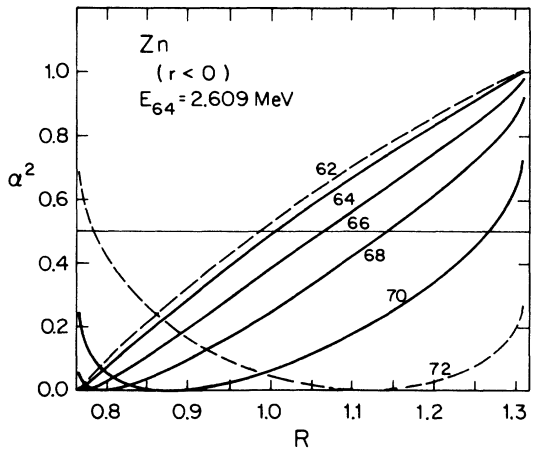

FIG. 11. Plot of α_A^2 vs R for $P_A<0$ and $T_A>0$ and r negative (using the 2.609-MeV state in ^{64}Zn).

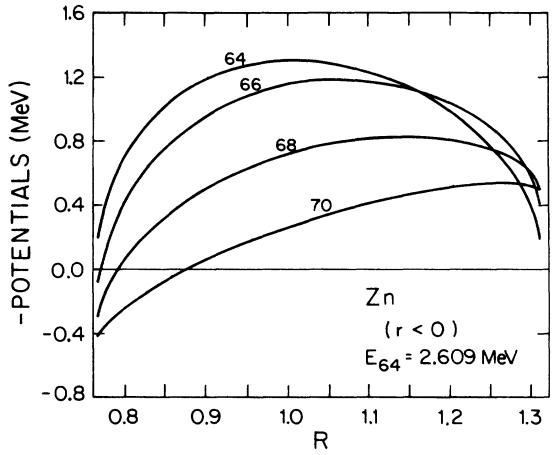

FIG. 12. Plot of $-U_A$ (in MeV) vs R for $P_A<0$ and $T_A>0$ and r negative (using the 2.609-MeV state in ^{64}Zn).

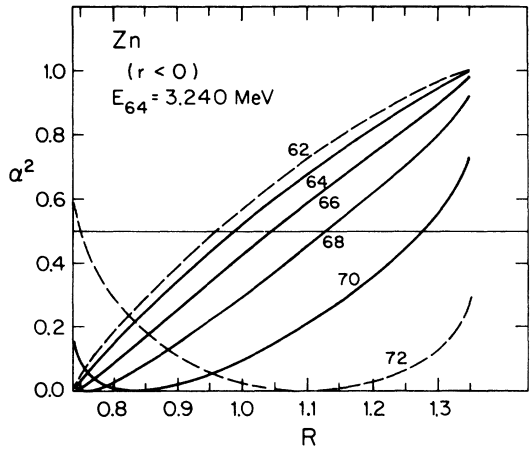

FIG. 13. Plot of α_A^2 vs R for $P_A<0$ and $T_A>0$ and r negative (using the 3.240-MeV state in ^{64}Zn).

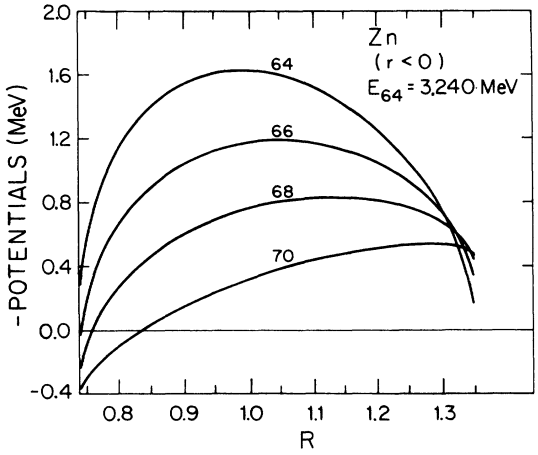

FIG. 14. Plot of $-U_A$ (in MeV) vs R for $P_A<0$ and $T_A>0$ and r negative (using the 3.240-MeV state in ^{64}Zn).

the 2.609-MeV calculation and $R=1.328$ for the 3.240-MeV calculation. The significant feature to notice is that in the 3.240-MeV calculation, almost all the potentials now intersect at $R\approx 1.328$ giving a common value of -0.54 MeV for U_A. However, the steepness of the mixing potentials around this R value indicates that a slight deviation in R could result in large changes in $-U_A(R)$.

V. $E2$ TRANSITIONS

The Rergl two-state model analysis as described above is capable of accounting for the $0^{+'}$/g.s. two-neutron cross-section ratio data in the even zinc isotopes. The two-state model wave functions are all described in terms of the one parameter R which is allowed to vary over a finite range of values. Of course, choosing a particular value of R is equivalent to making a specific choice of definition of basis states. As noted for the germanium analysis, one may be able to describe other direct-reaction data, e.g., proton occupation numbers[19] and alpha-transfer cross-section ratio data,[18] still without having to specify a unique value of R. Therefore, it is desirable to apply these Zn Rergl 0^+ wave functions to data that are not governed by a direct transfer mechanism, e.g., the electromagnetic transition rates. In this section, therefore, we consider the $E2$ rates in even zinc isotopes along with a set of assumed 2^+ wave functions to investigate possible choices of R.

A. Experimental $B(E2)$ data

Electromagnetic $B(E2)$ transition rates in the even zinc isotopes have been measured by many different groups[20–27] and are summarized in Refs. 28–30. To compare our zinc Rergl 0^+ wave functions to these data requires calculations of the *reduced* matrix element between the final and initial states. The experimental reduced matrix elements in the even zinc isotopes are obtained from the measured $B(E2)$ transition rates and the standard expression[31] [with $M(E2)$ in units of e fm^2],

$$B(E2;J_i\rightarrow J_f)=\frac{\langle J_f\|E2\|J_i\rangle^2}{(2J_i+1)}=\frac{[M(E2;J_i\rightarrow J_f)]^2}{(2J_i+1)}\ , \tag{8}$$

the results of which are summarized in Table VIII.

B. The 2^+ wave functions and the $E2$ reduced matrix elements

To calculate values for the reduced $E2$ matrix elements (and, hence, electromagnetic transition rates) requires that we form overlaps between 0^+ and 2^+ wave functions with the $E2$ operator sandwiched in between. In the Rergl analysis above, we have determined forms for the physical ground state and excited $0^{+'}$ state wave functions in ^{A}Zn.

In describing the two low-lying physical 2^+ states in

TABLE VIII. Experimental $B(E2)$ transition rates with the $E2$ matrix elements $|M(E2)|$. All data are summarized in Ref. 28 unless otherwise specified.

^{A}Zn	$J_i\rightarrow J_f$	$B(E2)$ (e^2fm^4)	$\|M(E2)\|$ (e fm^2)
^{62}Zn[a]	$2_1^+\rightarrow$g.s.	241±14	34.7±1.0
	$2_2^+\rightarrow$g.s.	4.8(+0.8, −0.6)	4.9(+0.4, −0.3)
^{64}Zn	$2_1^+\rightarrow$g.s.	316±10	39.75±0.63
	$0_2^+\rightarrow 2_1^+$	0.86±0.05[b]	0.93±0.03
	$2_2^+\rightarrow$g.s.	3.50±0.30	4.18±0.18
	$0_2^+\rightarrow 2_2^+$	935±120[b]	30.6±2.0
	$0_3^+\rightarrow 2_1^+$	133±37[b]	11.6±1.6
	$0_3^+\rightarrow 2_2^+$	$20<B(E2)<85$	$4.5<\|M(E2)\|<9.2$
^{66}Zn	$2_1^+\rightarrow$g.s.	274±10	37.0±0.7
	$0_2^+\rightarrow 2_1^+$	$B(E2)>2.0$[b]	$\|M(E2)\|>1.41$
	$2_2^+\rightarrow$g.s.	0.76±0.12	1.95±0.15
^{68}Zn	$2_1^+\rightarrow$g.s.	272±12	36.88±0.81
	$0_2^+\rightarrow 2_1^+$	125(+125, −45)[b]	11.2(+5.6, −2.0)
	$2_2^+\rightarrow$g.s.	8.9±1.6	6.67±0.06
	$2_2^+\rightarrow 0_2^+$	150±30	27,4±2.7
^{70}Zn	$2_1^+\rightarrow$g.s.	330±28	40.6±1.7
	$2_2^+\rightarrow$g.s.	10±2	7.07±0.71

[a]Reference 22.
[b]Reference 20.
[c]Reference 27.
[d]Reference 23.

zinc, we represent the 2^+ wave functions in ^{A}Zn also by a two-state mixing model and write

$$\Psi^A(2_1^+)=\gamma_A\phi_{2g}^A+\delta_A\phi_{2e}^A\ ,$$
$$\Psi^A(2_2^+)=\delta_A\phi_{2g}^A-\gamma_A\phi_{2e}^A\ , \tag{9}$$

with γ_A and δ_A real, $\gamma_A^2+\delta_A^2=1$ and ϕ_{2g}^A and ϕ_{2e}^A representing the 2^+ basis states.

To calculate the $B(E2)$ transition rates or the more symmetric, $M_A(E2;2_i^+\leftrightarrow 0_j^+)$ matrix element, we form the overlap $\langle\Psi^A(2_i^+)\|E2\|\Psi^A(0_j^+)\rangle$ which we denote by $M_A(2i0j)$ [see Fig. 15(a)]. This leads to the set of equations (in matrix form)

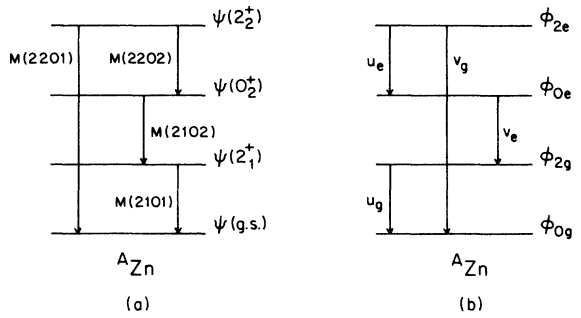

FIG. 15. (a) Schematic representation of the $M_A(2i0j)$ transition matrix elements between the physical states of ^{A}Zn. (b) Schematic representation of the $E2$ transition matrix elements between the basis states of ^{A}Zn.

$$\begin{bmatrix}M_A(2101)\\M_A(2102)\\M_A(2201)\\M_A(2202)\end{bmatrix}=\begin{bmatrix}\alpha_A\gamma_A & \alpha_A\delta_A & \beta_A\gamma_A & \beta_A\delta_A\\ \beta_A\gamma_A & \beta_A\delta_A & -\alpha_A\gamma_A & -\alpha_A\delta_A\\ \alpha_A\delta_A & -\alpha_A\gamma_A & \beta_A\delta_A & -\beta_A\gamma_A\\ \beta_A\delta_A & -\beta_A\gamma_A & -\alpha_A\delta_A & \alpha_A\gamma_A\end{bmatrix}\begin{bmatrix}u_{A_g}\\ v_{A_g}\\ v_{A_e}\\ u_{A_e}\end{bmatrix}\ , \tag{10}$$

where we denote the $E2$ reduced matrix elements between the basis states by u_{A_g}, v_{A_g}, v_{A_e}, and u_{A_e}, as depicted in Fig. 15(b). As matrices, $\overline{M}_A=\overline{\mathcal{T}}_A\overline{U}_A$ with $\overline{\mathcal{T}}_A^T\overline{\mathcal{T}}_A=\overline{I}$. The unitary property of the matrix $\overline{\mathcal{T}}_A$ leads immediately to the sum rule $\overline{M}_A^T\overline{M}_A=\overline{U}_A^T\overline{U}_A$ which, written out in its entirety, becomes

$$M_A^2(2101)+M_A^2(2102)+M_A^2(2201)+M_A^2(2202)=u_{A_g}^2+v_{A_g}^2+v_{A_e}^2+u_{A_e}^2\ , \tag{11a}$$

indicating that the total $E2$ strength is invariant under a change of basis. Another invariant, which is easily verified from Eq. (10), is given by the expression

$$M_A(2101)M_A(2202)-M_A(2102)M_A(2201)=u_{A_g}u_{A_e}-v_{A_g}v_{A_e}\ . \tag{11b}$$

The *total* $B(E2)$ strength from the 2^+ to the 0^+ states in this two-state mixing model represents a quantity which does not depend on the amount of 0^+ or 2^+ mixing in the basis states. It is possible to form other *partial* $B(E2)$ strengths that are independent of *only* 2^+ mixing or *only* 0^+ mixing. In particular, the sum of the $E2$ strengths leading only to the ground state or the sum of $E2$ strengths leading only to the excited $0^{+'}$ states are independent of the amount of 2^+ mixing and are given by

$$M_A^2(2101)+M_A^2(2201)=\alpha_A^2(u_{A_g}^2+v_{A_g}^2)+\beta_A^2(u_{A_e}^2+v_{A_e}^2)+2\alpha_A\beta_A(u_{A_g}v_{A_e}+u_{A_e}v_{A_g}) \tag{12a}$$

and

$$M_A^2(2102)+M_A^2(2202)=\beta_A^2(u_{A_g}^2+v_{A_g}^2)+\alpha_A^2(u_{A_e}^2+v_{A_e}^2)-2\alpha_A\beta_A(u_{A_g}v_{A_e}+u_{A_e}v_{A_g})\ . \tag{12b}$$

Similarly, the sum of $B(E2)$ strengths coming from only the 2_1^+ state or the sum of $B(E2)$ strengths coming from only the 2_2^+ state are independent of the amount of 0^+ mixing and are given by

$$M_A^2(2101)+M_A^2(2102)=\gamma_A^2(u_{A_g}^2+v_{A_e}^2)+\delta_A^2(u_{A_e}^2+v_{A_g}^2)+2\gamma_A\delta_A(u_{A_g}v_{A_g}+u_{A_e}v_{A_e}) \tag{13a}$$

and

$$M_A^2(2201)+M_A^2(2202)=\delta_A^2(u_{A_g}^2+v_{A_e}^2)+\gamma_A^2(u_{A_e}^2+v_{A_g}^2)-2\gamma_A\delta_A(u_{A_g}v_{A_g}+u_{A_e}v_{A_e})\ . \tag{13b}$$

VI. COLLECTIVE-MODEL LIMITS IN THE BASIS STATES

The large $B(E2)$ transition rates compared to the single-particle estimates in ^{A}Zn suggest collectivity in the basis states and two of the simplest types of collectivities are vibrational and rotational. We, therefore, shall consider calculations in which the basis states in ^{A}Zn are vibrational or rotational.

A vibrational spectrum contains two low-lying 0^+ and

two low-lying 2^+ states. However, in that case the second 2^+ level (a member of the two-phonon triplet) has no $E2$ decay to either of the two 0^+ states.[31] In the present notation, this requires $u_{A_e}=v_{A_g}=0$, which via Eq. (11b), demands that $M_A^2(2101)M_A^2(2202)=M_A^2(2102)M_A^2(2201)$. This condition is not satisfied by $E2$ data in ^{68}Zn because both $M_{68}^2(2101)$ and $M_{68}^2(2202)$ are large while both $M_{68}^2(2102)$ and $M_{68}^2(2201)$ are small. Therefore the vibrational-model limit in the zinc 0^+ and 2^+ basis states can be ruled out.

Hence, at least one $0^+,2^+$ pair must be other than vibrational. If they are true intruder states, they are likely members of a 0^+ rotational band. Then it is natural to assume that each of the low-lying 0^+ basis states is connected (via an $E2$ transition) to only one of the low-lying 2^+ states. We label this the NODME limit (no off-diagonal matrix elements). We therefore set $v_{A_g}=v_{A_e}=0$.

In this NODME limit the set of Eqs. (10) become

$$M_A(2101)=\alpha_A\gamma_A u_{A_g}+\beta_A\delta_A u_{A_e}\ , \tag{14a}$$

$$M_A(2102)=\beta_A\gamma_A u_{A_g}-\alpha_A\delta_A u_{A_e}\ , \tag{14b}$$

$$M_A(2201)=\alpha_A\delta_A u_{A_g}-\beta_A\gamma_A u_{A_e}\ , \tag{14c}$$

$$M_A(2202)=\beta_A\delta_A u_{A_g}+\alpha_A\gamma_A u_{A_e}\ , \tag{14d}$$

the set of Eqs. (11) become

$$M_A^2(2101)+M_A^2(2201)+M_A^2(2102)+M_A^2(2202)=u_{A_g}^2+u_{A_e}^2\ , \tag{15a}$$

$$M_A(2101)M_A(2202)-M_A(2102)M_A(2201)=u_{A_g}u_{A_e}\ , \tag{15b}$$

and the set of Eqs. (12) become

$$M_A^2(2101)+M_A^2(2201)=\alpha_A^2u_{A_g}^2+\beta_A^2u_{A_e}^2\ , \tag{16a}$$

$$M_A^2(2102)+M_A^2(2202)=\alpha_A^2u_{A_g}^2+\alpha_A^2u_{A_e}^2\ , \tag{16b}$$

$$M_A^2(2101)+M_A^2(2102)=\gamma_A^2u_{A_g}^2+\delta_A^2u_{A_e}^2\ , \tag{16c}$$

$$M_A^2(2201)+M_A^2(2202)=\delta_A^2u_{A_g}^2+\gamma_A^2u_{A_e}^2\ . \tag{16d}$$

To solve these equations for the 2^+ and 0^+ mixing, we subtract Eq. (16b) from (16a) to obtain

$$M_A^2(2101)-M_A^2(2102)+M_A^2(2201)-M_A^2(2202)=(\alpha_A^2-\beta_A^2)(u_{A_g}^2-u_{A_e}^2)\ . \tag{17a}$$

In addition, Eqs. (14a)–(14d) combine to yield

$$M_A(2101)M_A(2102)+M_A(2201)M_A(2202)=\alpha_A\beta_A(u_{A_g}^2-u_{A_e}^2)\ . \tag{17b}$$

Finally, these two equations coupled together lead to

$$\alpha_A^2-Q_A\alpha_A\beta_A-\beta_A^2=0 \tag{18a}$$

with

$$Q_A=\frac{M_A^2(2101)-M_A^2(2102)+M_A^2(2201)-M_A^2(2202)}{M_A(2101)M_A(2102)+M_A(2201)M_A(2202)}\ , \tag{18b}$$

A similar set of steps also leads to the 2^+ mixing probabilities satisfying

$$\gamma_A^2-S_A\gamma_A\delta_A-\delta_A^2=0 \tag{19a}$$

with

$$S_A=\frac{M_A^2(2101)-M_A^2(2201)+M_A^2(2102)-M_A^2(2202)}{M_A(2101)M_A(2201)+M_A(2102)M_A(2202)}\ . \tag{19b}$$

In terms of the ratios, $x_A=\alpha_A/\beta_A$ and $y_A=\gamma_A/\delta_A$, Eqs. (18a) and (19a) become

$$x_A^2-Q_Ax_A-1=0 \tag{20}$$

and

$$y_A^2-S_Ay_A-1=0\ . \tag{21}$$

Using the fact that we can physically require x_A and y_A to be non-negative leads to the *unique* amplitude ratios given by

$$x_A=(\tfrac{1}{2})[Q_A+(Q_A^2+4)^{1/2}] \tag{22}$$

and

$$y_A=(\tfrac{1}{2})[S_A+(S_A^2+4)^{1/2}]\ . \tag{23}$$

Therefore the $E2$ transition rates in ^{A}Zn, assuming two-state mixing and the NODME limit in the 0^+ and 2^+ basis states, lead to unique values for the 0^+ and 2^+ mixing probabilities, α_A^2 and γ_A^2, and, hence, a unique value for R.

It should be noted that the expressions given by Eqs. (22) and (23) result from Eqs. (16a)–(16d) which are relationships between the *squares* of $M_A(2i0j)$, α_A, γ_A, u_{A_g}, and u_{A_e}. These values of x_A and y_A may not necessarily satisfy all of Eqs. (14a)–(14d), which are *linear* in $M_A(2i0j)$, α_A, γ_A, u_{A_g}, and u_{A_e}. There exists, in fact, a connecting equation that the mixing-amplitude ratios given by Eqs. (22) and (23) must satisfy. To obtain this relationship, we combine Eqs. (14a) and (14b) yielding the set of equations

$$\beta_AM_A(2102)+\alpha_AM_A(2101)=\gamma_Au_{A_g}\ , \tag{24a}$$

$$\beta_AM_A(2202)+\alpha_AM_A(2201)=\delta_Au_{A_g}\ , \tag{24b}$$

$$\beta_AM_A(2101)-\alpha_AM_A(2102)=\delta_Au_{A_e}\ , \tag{24c}$$

$$\alpha_AM_A(2202)-\beta_AM_A(2201)=\gamma_Au_{A_e}\ , \tag{24d}$$

which together imply

$$y_A=\frac{M_A(2102)+x_A M_A(2101)}{M_A(2202)+x_A M_A(2201)} \tag{25a}$$

and

$$y_A=\frac{x_A M_A(2202)-M_A(2201)}{M_A(2101)-x_A M_A(2102)} . \tag{25b}$$

In addition, Eqs. (24) combine to yield the basis state $E2$ transition-rate matrix elements

$$u_{A_g}=\alpha_A\gamma_A M_A(2101)+\beta_A\gamma_A M_A(2102)+\alpha_A\delta_A M_A(2201)+\beta_A\delta_A M_A(2202)$$

and (26)

$$u_{A_e}=\beta_A\delta_A M_A(2101)-\alpha_A\delta_A M_A(2102)-\beta_A\gamma_A M_A(2201)+\alpha_A\gamma_A M_A(2202) .$$

Using Eq. (22) to obtain the 0^+ mixing, Eq. (25a) (with $y_A\geq 0$) to obtain the 2^+ mixing and Eqs. (26) to obtain the $E2$ reduced matrix elements connecting the basis states will yield x_A, y_A [and, hence, $\alpha_A^2=x_A^2/(1+x_A^2)$ and $\gamma_A^2=y_A^2/(1+y_A^2)$], u_{A_g}, and u_{A_e} that satisfy all of Eqs. (14a)–(14d).

VII. APPLICATIONS TO ^{68}Zn

It is clear from Eqs. (18b), (21), and (25a) that four physical $E2$ transition rates between 2_i^+ and 0_j^+ $(i,j=1,2)$ are needed in order to calculate mixing amplitudes between the 0^+ and 2^+ basis states as described above in the NODME limit. In all the zinc isotopes, except for ^{64}Zn and ^{68}Zn, the experimental $B(E2)$ data are not complete (Table VIII) enough to apply this analysis. In ^{64}Zn, enough data exist provided we assume that it is the 0_2^+ state that is mixed with the ground state in the Rerg1 analysis. However, the excitation energy trend with A and Fig. 14 favors the 0_4^+ state in ^{64}Zn as the proper mixed excited $0^{+'}$ state. If we assume that this is so then there does not exist enough $E2$ transition-rate data for the NODME limit $E2$ analysis in ^{64}Zn. Thus we apply the model only to ^{68}Zn.

Since it is the $E2$ "amplitude" ratios that determine Q_{68} in Eq. (18b) and, hence, x_{68} in Eq. (22), we must consider all 16 possible sign combinations in the four $E2$ experimental matrix elements. Of these 16, eight of them lead to negative y_{68} [via Eq. (25a)] values and may, therefore, be dismissed. The remaining eight solutions (labeled A–H) are tabulated in Table IX where the following observations can be noted: (1) both $M_{68}(2101)$ and $M_{68}(2202)$ must have the same sign in all cases, (2) the eight solutions occur in two sets of four with one set having u_g and u_e positive and another with them negative, and (3) in each set of four solutions, the elements occur in two sets of two that are related by the transformation, $M_{68}(2101)\leftrightarrow M_{68}(2101)$, $M_{68}(2202)\leftrightarrow M_{68}(2202)$, $M_{68}(2102)\leftrightarrow -M_{68}(2102)$, $M_{68}(2201)\leftrightarrow -M_{68}(2201)$, $\alpha_{68}^2\leftrightarrow\beta_{68}^2$, $\gamma_{68}^2\leftrightarrow\delta_{68}^2$, and $u_g\leftrightarrow u_e$. Thus there are only two "independent" solutions which are labeled by A and B in Table IX.

In both calculations A and B, we find that u_{68_g} is larger than u_{68_e} by factors of 1.9 and 1.4, respectively. Also in solution B, we find almost no mixing in the ^{68}Zn 2^+ basis states. In fact, within the uncertainties in the ^{68}Zn $B(E2)$ data, $\gamma_{68}^2=1$ is consistent with calculation B in Table IX.

VIII. 0^+ MIXING AMPLITUDES IN THE EVEN ZINC ISOTOPES

The 0^+ and 2^+ mixing amplitudes in ^{68}Zn have been determined above using only the $E2$ transition-rate data. If we incorporate this 0^+ mixing probability in ^{68}Zn with the Rerg1 results of Fig. 13, then we can determine a unique value for the Rerg1 parameter R, and hence the 0^+ mixing probabilities, α_A^2 and 0^+ mixing potentials $-U_A$ in all even zinc isotopes. These are given for $^{64-70}$Zn, with error bars, in Table X for the α_{68}^2 values resulting from the four $E2$ calculations A, B, C, and D in Table IX. The results are also plotted versus mass number in Figs. 16–19. We do not consider ^{62}Zn and ^{72}Zn because the 0^+ mixing probabilities for these are not uniquely determined by the Rerg1 analysis (see dashed curves in Fig. 13).

The results of calculation A give $R=1.251\pm0.032$ and

TABLE IX. The calculated values of α_{68}^2, γ_{68}^2, u_{68_g}, and u_{68_e} using the ^{68}Zn $B(E2)$ transition-rate data and the NODME limit in the basis states for those sign combinations in $M_{68}(2i0j)$ consistent with x_{68} and y_{68} non-negative.[a] The sign combination order is for $M_{68}(2101)$, $M_{68}(2102)$, $M_{68}(2201)$, and $M_{68}(2202)$.

Calc.	Sign combinations				α_{68}^2	γ_{68}^2	u_{68_g} (e fm^2)	u_{68_e} (e fm^2)
A	+	+	+	+	0.7027	0.7648	42.33	22.11
B	+	+	−	+	0.8769	0.9924	38.61	28.11
C	+	−	+	+	0.1231	0.0076	28.11	38.61
D	+	−	−	+	0.2973	0.2352	22.11	42.33
E	−	+	+	−	0.2973	0.2352	−22.11	−42.33
F	−	+	−	−	0.1231	0.0076	−28.11	−38.61
G	−	−	+	−	0.8769	0.9924	−38.61	−28.11
H	−	−	−	−	0.7027	0.7648	−42.33	−22.11

[a]Using Eqs. (22), (25a), and (26) in the text.

TABLE X. The 0^+ mixing probabilities and mixing potentials determined from the $B(E2)$ electromagnetic transition-rate and two-neutron transfer data using calculations A and B from Table IX.

	Calculation A		Calculation B	
	$\gamma^2_{68}=0.765\pm0.057$ $-U_{68}(2^+)=0.342\pm0.058$ MeV $u_{68_g}=42.33\pm2.84$ e fm^2 $u_{68_e}=22.11\pm3.04$ e fm^2 $R=1.251\pm0.032$		$\gamma^2_{68}=0.992\pm0.008$ $-U_{68}(2^+)=0.070\pm0.070$ MeV $u_{68_g}=38.61\pm2.04$ e fm^2 $u_{68_e}=28.11\pm2.57$ e fm^2 $R=1.327\pm0.027$	
A	α^2_A	$-U_A$ (MeV)	α^2_A	$-U_A$ (MeV)
64	0.883±0.041	1.041±0.159	0.971±0.029	0.540±0.540
66	0.817±0.049	0.917±0.097	0.941±0.050	0.558±0.259
68	0.703±0.058	0.757±0.043	0.877±0.084	0.544±0.128
70	0.448±0.063	0.532±0.007	0.663±0.113	0.506±0.122
	Calculation C		Calculation D	
	$\gamma^2_{68}=0.008\pm0.008$ $-U_{68}(2^+)=0.070\pm0.070$ MeV $u_{68_g}=28.11\pm2.57$ e fm^2 $u_{68_e}=38.61\pm2.04$ e fm^2 $R=0.890\pm0.051$		$\gamma^2_{68}=0.235\pm0.057$ $-U_{68}(2^+)=0.342\pm0.058$ MeV $u_{68_g}=22.11\pm3.04$ e fm^2 $u_{68_e}=42.33\pm2.84$ e fm^2 $R=1.001\pm0.038$	
A	α^2_A	$-U_A$ (MeV)	α^2_A	$-U_A$ (MeV)
64	0.321±0.097	1.513±0.123	0.520±0.064	1.619±0.008
66	0.239±0.088	1.011±0.131	0.426±0.063	1.172±0.023
68	0.123±0.084	0.544±0.128	0.297±0.058	0.757±0.043
70	0.022±0.022	0.155±0.155	0.097±0.037	0.317±0.055

show a monotonic drop in α^2_A as a function of A (Fig. 16). Similarly, for the 0^+ mixing potentials (Fig. 17). We note that the uncertainty for the $-U_{70}$ calculation at $R\approx1.251$ is very small and is due to the fact that at this R value, the function $-U_{70}(R)$ is very flat and near its maximum value of 0.538 MeV (see Fig. 14).

Calculation B gives $R=1.327\pm0.027$ and also shows a monotonic drop in α^2_A as a function of A (Fig. 18). The 0^+ mixing potentials at $R\approx1.327$ (Fig. 19), within the uncertainty of the calculation, are almost all equal. This result was also noted in Sec. IV B.

Calculation C, of course, has α^2_{68}(calculation C)

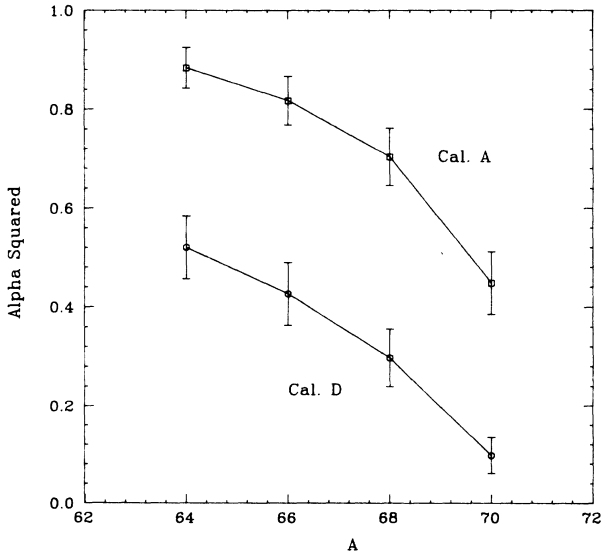

FIG. 16. Plot of α^2_A vs A using the ^{68}Zn mixing probability determined from the $E2$ transition-rate data in ^{68}Zn (calculations A and D).

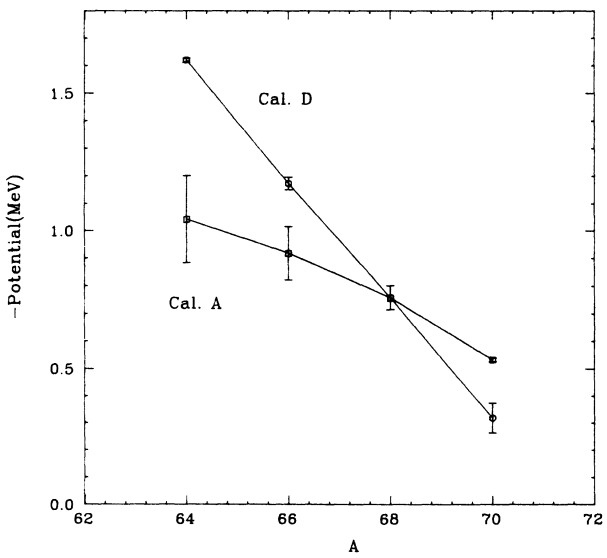

FIG. 17. Plot of $-U_A$ (MeV) vs A using the ^{68}Zn mixing probability determined from the $E2$ transition-rate data in ^{68}Zn (calculations A and D).

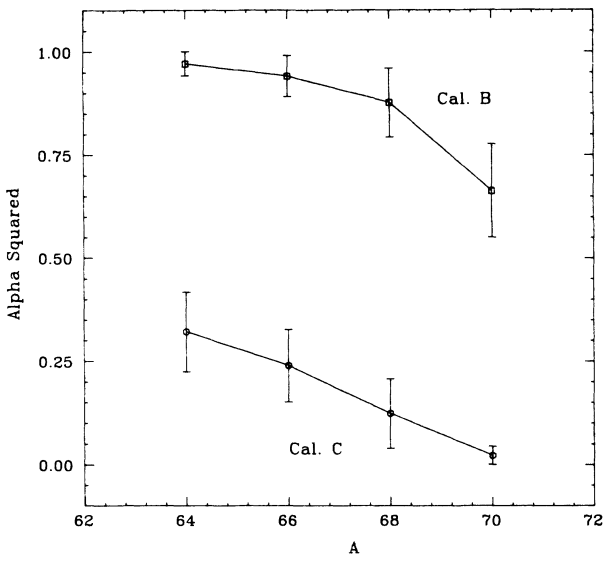

FIG. 18. Plot of α_A^2 vs A using the ^{68}Zn mixing probability determined from the $E2$ transition-rate data in ^{68}Zn (calculations B and C).

$=\beta_{68}^2$(calculation B) and γ_{68}^2(calculation C)$=\delta_{68}^2$(calculation B); and, hence, the 0^+ and 2^+ mixing potentials in ^{68}Zn are the same as in calculation B (but not, of course, in the other isotopes). The value for the basis-state $2n$-transfer overlap ratio R is 0.8897 ± 0.0510 and at this R value (Figs. 18 and 19), both the α_A^2's and $-U_A$'s decrease linearly with mass number A.

As with calculation C, calculation D is related to calculation A via α_{68}^2(calculation D)$=\beta_{68}^2$(calculation A) and γ_{68}^2(calculation D)$=\delta_{68}^2$(calculation A) and so the

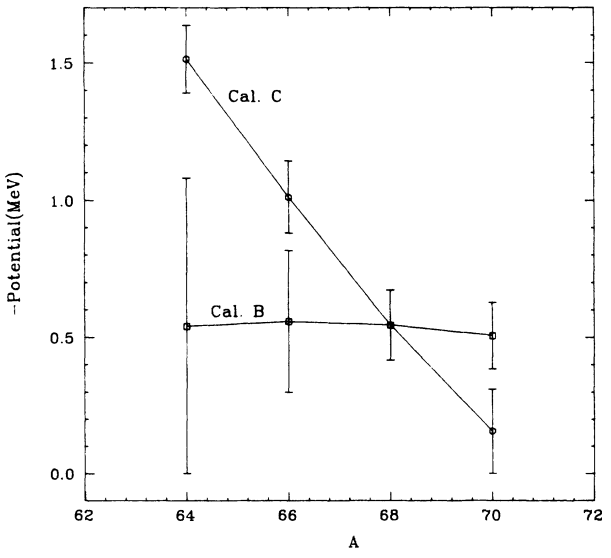

FIG. 19. Plot of $-U_A$ (MeV) vs A using the ^{68}Zn mixing probability determined from the $E2$ transition-rate data in ^{68}Zn (calculations B and C).

0^+ and 2^+ mixing potentials in ^{68}Zn for calculation D are the same as in calculation A. The value for the basis-state $2n$-transfer overlap ratio R is very nearly unity (1.0010 ± 0.0384). At this R value, the 0^+ mixing probabilities (Fig. 16) decrease monotonically with A and similarly, the 0^+ mixing potentials decrease with A and are linear (Fig. 17).

IX. SUMMARY AND CONCLUSIONS

We have measured the $\sigma(0_2^+)/\sigma$(g.s.) ratio in ^{70}Zn(p,t)^{68}Zn and used this result and other existing data to perform a generalized two-state coexistence (Rergl) analysis on zinc as was done for germanium. This two-state analysis on the ground state and first excited 0^+ state in the even-even zinc isotopes has been shown to account for the $2n$ stripping and pickup $\sigma(0_2^+)/\sigma$(g.s.) ratios without having to assume much about the nature of the initial- and final-state wave functions. This is in contrast to a shell-model analysis of two-nucleon transfer data which is very dependent on the form of the initial- and final-state wave functions.

The results of the Rergl analysis show that the wave functions for the heavier zinc isotopes (i.e., for ^{70}Zn and ^{72}Zn) are different from those of the lighter ones with the transition occurring at about $N=40$. This is consistent with previous measurements and calculations as determined in Refs. 2–4, and 18. Our calculations do however, seem to favor a small destructively interfering term in $2n$-transfer overlaps between the ground states of the zinc isotopes (to the extent that r is small and negative).

For each calculation considered, there exists an R region for which the mixing potentials are all about equal to -0.5 MeV, especially when the 3.240-MeV state in ^{64}Zn is used as the $0^{+\prime}$ state instead of the 1.910-MeV state. This, however, is not a sufficient requirement to determine the value of R nor to determine the correct mixed excited 0^+ state in ^{64}Zn.

We have taken these 0^+ wave functions, along with an assumed set of two-state mixed 2^+ wave functions, and applied them to fitting the $E2$ transition-rate data in the even zinc isotopes. The fact that these transition rates are so large suggests collectivity in the basis states and we have considered both vibrational and rotational collectivity. Assuming a vibrational-model limit in the basis states leads to an inconsistency between the model and the experimental $E2$ data in ^{68}Zn. However, with no off-diagonal matrix elements between the basis states, the $E2$ data allow for the determination of the 0^+ and 2^+ mixing probabilities in ^{68}Zn. There exists (Table IX) two independent sets of mixing probabilities consistent with the $E2$ transition-rate data in ^{68}Zn.

Knowledge of the 0^+ mixing probability in one zinc nucleus allows for the determination of all 0^+ mixing probabilities in the other even zinc nuclei because the value of the Rergl parameter R may be determined. The results of these calculations (using the α_A^2's and $-U_A$'s of Figs. 13 and 14) are given in Table X. We note that for calculations B and C of that table, the 2^+ states in ^{68}Zn are nearly pure. For calculation B, the 0^+ mixing potentials are nearly independent of mass num-

ber A while for calculation C, the 0^+ mixing potentials decrease linearly with mass number. Calculation D has $R \approx 1.00$ and 0^+ mixing probabilities that decrease linearly with A. Furthermore, the 2^+ mixing potential is very nearly $1/\sqrt{5}$ times that for 0^+ in calculation D, as one might expect in some models of the basis states.

Quantitatively checking these Rergl 0^+ and 2^+ wave functions with other data (e.g., precise proton occupation numbers as was done for germanium[19] or more electromagnetic transition-rate data in the other zinc isotopes) may confirm these mixing probabilities and may identify which state in ^{64}Zn is mixed with the ground state in a two-state model.

We acknowledge financial support from the National Science Foundation.

---

*Present address: Department of Physics and Atmospheric Sciences, Drexel University, Philadelphia, PA 19104.

[1]P. J. Brussaard and P. W. M. Glaudemans, *Shell-Model Applications in Nuclear Spectroscopy* (North-Holland, Amsterdam, 1977).
[2]M. Carchidi and H. T. Fortune, J. Math. Phys. **27**(2), 633 (1986).
[3]M. Carchidi, H. T. Fortune, G. S. F. Stephens, and L. C. Bland, Phys. Rev. C **30**, 1293 (1984).
[4]M. Vergnes, Inst. Phys. Conf. Ser. **49**, 25 (1980).
[5]A. M. Van den Berg *et al.*, Nucl. Phys. **A429**, 1 (1984).
[6]K. Heyde *et al.*, Phys. Rep. **102**, 291 (1983).
[7]J. F. A. Van Hienen, W. Chung, and B. H. Wildenthanl, Nucl. Phys. **A269**, 159 (1976).
[8]J. E. Koops and P. W. M. Glaudemans, Z. Phys. A **280**, 181 (1977).
[9]*Table of Isotopes,* 7th ed., edited by C. Michael Lederer and Virginia Shirley (Wiley, New York, 1978).
[10]Hideshige Kusakari *et al.*, J. Phys. Soc. Jpn. **34**, 865 (1973).
[11]R. A. Hinrichs and D. M. Patterson, Phys. Rev. C **10**, 1381 (1974).
[12]F. R. Hudson and R. N. Glover, Nucl. Phys. **A189**, 264 (1972).
[13]L. C. Farwell, J. J. Kraushaar, and H. W. Baer, Nucl. Phys. **A186**, 545 (1972).
[14]L. C. McIntyre, Phys. Rev. **152**, 1013 (1966).
[15]M. Carchidi *et al.* (unpublished).
[16]P. D. Kunz (private communication).
[17]Shiro Yoshida, Nucl. Phys. **33**, 685 (1962).
[18]M. Carchidi and H. T. Fortune, Phys. Rev. C **31**, 853 (1985).
[19]H. T. Fortune, M. Carchidi, and S. Mordechai, Phys. Lett. **145B**, 4 (1984).
[20]A. Passoja *et al.*, Nucl. Phys. **A438**, 413 (1985).
[21]A. Passoja *et al.*, Phys. Lett. **124B**, 157 (1983).
[22]N. J. Ward *et al.*, J. Phys. G **7**, 815 (1981).
[23]P. M. Endt, At. Data Tables **23**, 547 (1979), and references therein.
[24]D. N. Simister *et al.*, J. Phys. G. **4**, 111 (1978).
[25]D. N. Simister *et al.*, J. Phys. G. **4**, 1127 (1978).
[26]D. N. Simister *et al.*, J. Phys. G. **6**, 81 (1980).
[27]R. Neuhausen, Habilitationschrift, Institut für Kernphysik, Universität Mainz, Report No. KPH 22/74, 1974 (unpublished).
[28]C. H. Druce, J. D. McCullen, P. D. Duval, and B. R. Barrett, J. Phys. G **8**, 1565 (1982).
[29]Mitsuo Sakai, At. Data Nucl. Data Tables **31**, 399 (1984), and references therein.
[30]S. Raman *et al.*, At. Data Nucl. Data Tables **36**, 1 (1987), and references therein.
[31]D. J. Rowe, *Nuclear Collective Motion: Models and Theory* (Methuen, London, 1970), p. 21.